# Operational vibration of a waterjet focuser as means for monitoring its wear progression

Edoardo Copertaro, Francesco Perotti, Massimiliano Annoni
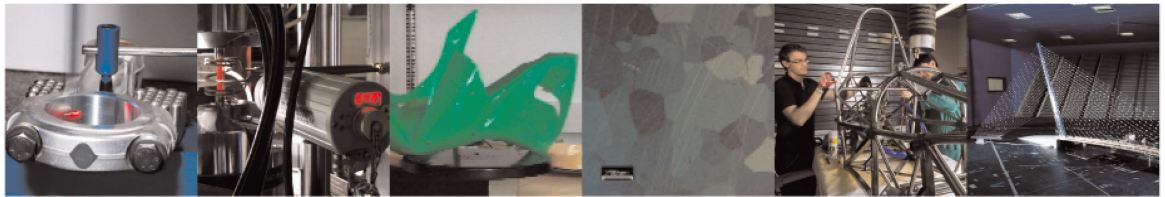
# Operational vibration of a waterjet focuser as means for monitoring its wear progression

Edoardo Copertaro [a], Francesco Perotti[b], Massimiliano Annoni [b]


(a)     *Université du Luxembourg, Faculté des Sciences, de la Technologie et de la Communication, Avenue de l'Université, L-4365, Esch-sur-Alzette, Luxembourg*

(b)     *Politecnico di Milano, Dipartimento di Meccanica, Via Privata Giuseppe La Masa 1, 20156, Milano, Italia*


**Corresponding author**     Edoardo Copertaro

**Contact details**     Postal address:     12, Rue Ancienne Cote d'Eich, 1459, Luxembourg Ville (L)

Email:     edoardo.copertaro@uni.lu

Office:     + 352 466 644 6836

Fax:     + 352 466 644 35790

Mobile 1:     + 39 338 658 1667

Mobile 2:     + 352 661 369 501

## Abstract

Abrasive waterjet cutting is a competitive manufacturing technology in the aerospace, defense and automotive industries. End-user requirements are currently pushing machine builders to improve the automation of their processes, in an effort to reduce costs and downtimes, as well as increase robustness and stability. On this regard, the waterjet focuser is a critical component, as its fast wear progression requires constant human supervision, for promptly detecting detrimental effects on the cutting performance. This paper describes an innovative approach for in-line monitoring the wear progression of a waterjet focuser, by means of an accelerometer installed on its tip. This result is allowed by two separate studies of the focuser, of which the first investigates the sensitivity of its first mode frequency to the wear progression, whilst the second demonstrates the possibility of tracking said frequency from the in-line vibration signal delivered by the accelerometer, during operation. The presented setup makes use of low-cost sensing hardware that can be easily retrofitted into the design of waterjet focusers. The information delivered is expected to tackle end-user requirements for improved process automation.

## Keywords

Abrasive Waterjet Cutting; Predictive Maintenance; Process Monitoring; Vibration Measurements.

**Introduction**

Abrasive Waterjet Cutting (AWJC) as a manufacturing technology has been the object of investigation since the early 1960s [1]. Established sources can provide frame of reference and give a deep insight into this technology and its applications [2][3][4][5]. The aerospace, defense and automotive industries constitute the largest end-user segments of AWJC [6]; here, several features contribute to provide an edge with respect to alternative manufacturing technologies, notably lower initial investment, absence of a heat-affected zone on the workpiece, no limitations in shape complexity, no mechanical contact with physical tools, narrow kerf (down to 0.3 mm), negligible blurs, good edge sharpness [5][7]. However, tight quality standards of said reference sectors, as well as high operating costs of AWJC [6], pose a challenge to machine builders for improving the automation and stability of their processes; on this regard, their efforts have been pushed in the direction of delivering enhanced components, more robust and reliable [1], as well as developing new techniques for process monitoring [8]. The improvement of AWJC automation constitutes the driver of the present research, which lies in the field of vibroacoustic process monitoring as means for extracting relevant information that could be beneficial for the purpose.

Figure 1 shows the cutting head of an AWJC system: here water flows through the primary orifice at very high pressure, up to 600 MPa; the primary orifice performs a conversion of pressure into kinetic energy, which results in a high-speed (about 1000 m/s) waterjet; abrasive particles are fed with air into the mixing chamber; the resulting abrasive jet travels through the focuser and momentum is transferred to the particles, which are consequently accelerated; finally, the abrasive jet exits the focuser, gets airborne, then impinges on the workpiece, producing the removal of material.

The focuser constitutes a critical part of an AWJC system; the component is made of hard tungsten carbide or boron carbide and its inner diameter typically ranges between 0.5 mm and 2.0 mm [1]; its primary scope is stabilizing the flow formed inside the mixing chamber, transferring momentum to the abrasive particles, and creating a focused, consistent, high-velocity, particle-laden abrasive jet [10]. However, the same focuser is the main target of an aggressive erosive action from the abrasive jet [3][11][12], which produces a progressive wear of its bore, according to an uneven waves profile [13][14]; the severity of such phenomenon limits its operational life to about 100 hours [1]; besides, it affects the momentum transfer's efficiency. Currently, there is no reliable, in-line technique available for monitoring the focuser's wear status [15]; hence, the common practice relies on periodic, visual inspections of the operator [16]; these even become mandatory, before machining delicate or expensive parts [10]. Overall, the requirement for constant human supervision impacts dramatically on operating costs, which reach up to 60 USD/h [6][17] and constitute the main weakness of AWJC with respect to alternative technologies, notably plasma and laser cutting, which do not exceed 20 USD/h [18][19]; moreover, such manual practice negatively affects process downtimes, as it requires a dedicated procedure; also, its reliability is dependent upon the operator's skills. Hence, the research has been pushed towards the development of automated and in-line monitoring techniques of the focuser's wear status; the following part of this section presents a literature survey on the subject.

A first group of techniques deals with the off-line inspection of the focuser's wear pattern. Here the most common method is to measure the inner profile over a certain period; this technique was used in [11] and allowed the author to produce relevant conclusions about the wear mechanisms taking place. Further off-line techniques are reported in [12] and include x-ray radiography, producing castings of the inner diameter by means of silicon resins, introducing progressively larger gage pins through the focuser's inner hole. Undoubtedly, off-line techniques represent effective tools for investigating the wear mechanisms and are commonly exploited for research and design optimization; however, the impossibility of using them in-line is straightforward.

The deployment of in-line techniques for monitoring the focuser's wear status conflicts with the inner harsh environment, the latter preventing the introduction of measurement probes inside the cutting head [10]; however, the possibility of using optical techniques to the scope has been investigated in the past. In [20], the authors used an infrared camera (FLIR SC3000), for monitoring the focuser's temperature during operation; results indicate a regime temperature of about 75 ℃ and a sensitivity of approximately 5 ℃ to the presence of defects, either in the focuser or in the primary orifice. A second optical setup is also discussed in [20], which makes use of a fast camera (PHOTRON SA5) for high-speed recordings (up to 500 frames per second) of the airborne jet; however, results are conflicting, and conclusions could not be made.

In [16], a new focuser's design is presented, in which concentric electric loops are embedded into its tip. By means of such embodiment, the focuser's wear status can be tracked in-line, by the closed or open status of each loop. Indeed, the system proved of being capable of in-line tracking the focuser's inner diameter, also providing the wear

propagation's direction, as well as delivering adequate information to the controller, for compensating the detrimental effect of the wear progression on the cutting performance.

Vibroacoustic diagnostics includes a wide range of methods and techniques, for assessing the status of general machinery [21]. Their notable advantages include the relatively low cost of sensors, non-invasiveness, compatibility with day-to-day operations and capability of delivering robust in-line estimators of target variables, during operation. The vibroacoustic emission has been used by different authors, for in-line monitoring of AWJC processes; the literature shows that a first category of methods deals with the monitoring of process and workpiece parameters, whilst a second category is related to the diagnostics and condition monitoring of the machine components. According to [3], the vibroacoustic emission of an AWJC system is correlated with the wear status of its components, in particular the primary orifice and the focuser.

In [15], the authors monitored the vibration of the workpiece, during AWJC operations. The monitoring setup included four accelerometers, installed on the workpiece. Two focusers were considered, with inner diameters of 0.8 mm and 1.4 mm. Signals were gathered at a sampling frequency of 30 kHz, then processed by means of a Fourier Transform. Figure 2 shows a comparison of the power spectra obtained with the two focusers, whilst the other process parameters were maintained constant. These results allowed the authors to conclude that the focuser's inner diameter has an impact on both the amplitude and frequency distribution of the vibration energy generated from the workpiece: as the inner diameter increases, the peaks of the spectra seem to reduce in amplitude and shift towards higher frequencies.

In [22], the operational acoustic emission of an AWJC apparatus was monitored by means of a condenser microphone, placed in the near field of the machinery. Three focusers were considered, with different inner diameters: 1.09 mm; 1.40 mm; 1.65 mm. Acoustic signals were gathered during firings of the waterjet and without cutting operation. The subsequent data processing included the computation of an Auto-Regressive Moving-Average (ARMA) estimate of the time signals, and subsequently a Fourier Transform of the ARMA estimations. Figure 3 compares the power spectra obtained with the different focusers and these results allowed the following conclusions: the ARMA spectra show two dominant frequency ranges, notably above and below 20 kHz; as the focuser's inner diameter increases, the spectra tend to shift towards higher frequencies; the signal's amplitude in the high frequency range appears to be a good indicator of the focuser's inner diameter. Analogous acoustic studies from the same author are also reported in [23][24].

According to the presented literature survey, vibroacoustic methods for in-line monitoring the focuser's wear status seem to fall into two categories: those relying on vibration sensors installed on the workpiece, which exploit the correlation of its vibration with the force produced by the impinging jet and in turn with the focuser's status; those based on the monitoring of the acoustic field and the extraction of relevant features from the gathered signals. Regarding the first category, these methods have the relevant drawback of requiring mounting and dismounting of the sensing hardware at each workpiece replacement, with a consequent negative impact on both the measurement reproducibility and process downtimes. Regarding the second category, acoustic measures suffer environmental interferences and for such reason their deployment is always a tricky task, especially in industrial scenarios.

A further consideration on the state of the art regards the substantial absence of a modal study of the systems involved, which could provide a solid basis for the deterministic analysis of the gathered signals; instead, their interpretation has been reduced so far to a pure exercise of pattern recognition, whilst the robustness and reproducibility of such fuzzy approach has never been addressed. On this regard, the authors have already demonstrated that vibration energy generated during AWJC operations includes relevant contributions up to 50 kHz and beyond [25]. Given such a wide frequency range, the impact of the focuser's wear on frequency-localized contributions tends to go unnoticed. The present study is an application of measurement science and structural dynamics to the solution of a technological problem. It is proven how such transversal approach can deliver an a-priori identification of relevant vibration contributions for the purpose of the focuser's wear tracking, thus enabling a more robust and effective signals' analysis. Indeed, the present study takes the steps from the limits of the state of the art and is intended to deliver an improved method that: i) does not entail sensors on the workpiece; ii) is based on structure-borne vibration sensors, hence can provide adequate robustness for its deployment in a real production environment; iii) exploits a deterministic approach for extracting a robust indicator of the focuser's wear status, from the vibration signal. This result is delivered by means of two separate studies, of which the first investigates the sensitivity of the focuser's mode frequencies to its wear progression, whilst the second demonstrates the possibility of in-line tracking the first of said frequencies during operation, by means of the signal delivered by a micro accelerometer installed at the focuser's tip. Overall, the presented method appears effective in delivering a robust in-line indicator of the focuser's wear status. The monitoring hardware is compatible with day-to-day operations and its installation only requires a minor focuser's redesign. The

information delivered is expected to overcome the requirement for constant human supervision over the focuser's wear status; besides, the innovative wear indicator could be used analogously to [16], as the observed variable of a head position's control loop that is intended to compensate the detrimental effect of wear progression on the cutting accuracy.

The present contribution is structured as follows: Section 2 presents the background theory of modal analysis; Section 3 presents the focuser's modal study, which is intended to characterize its vibration modes and assess their sensitivities to the wear progression; Section 4 presents the second study, which demonstrates the possibility of in-line monitoring the first mode frequency during operation, by means of one on-board accelerometer; Section 5 draws the conclusions of the work.
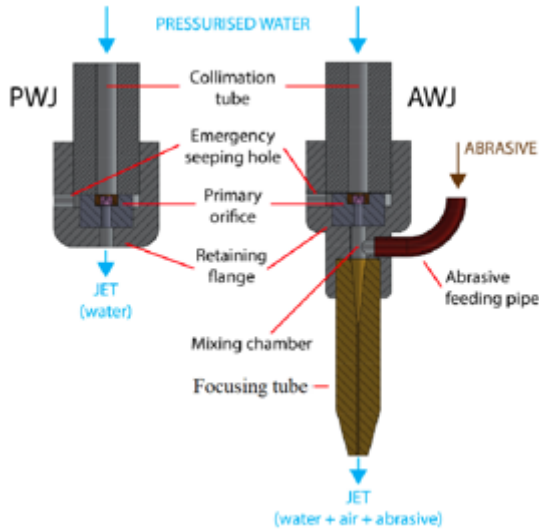


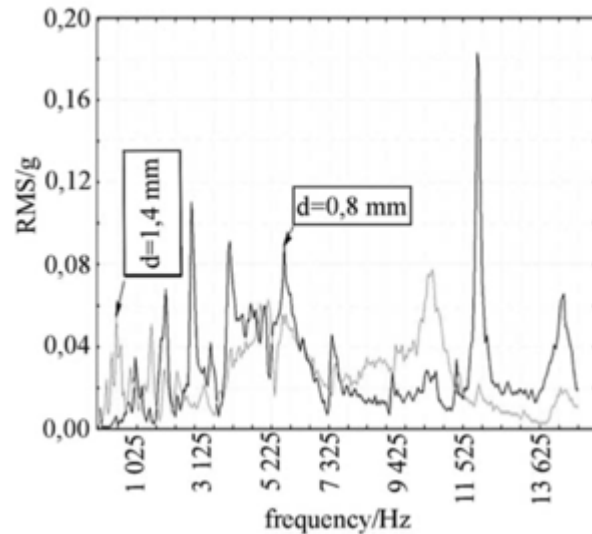**Figure 1. AWJC head (PWJ: pure waterjet; AWJ: abrasive waterjet) [9].**



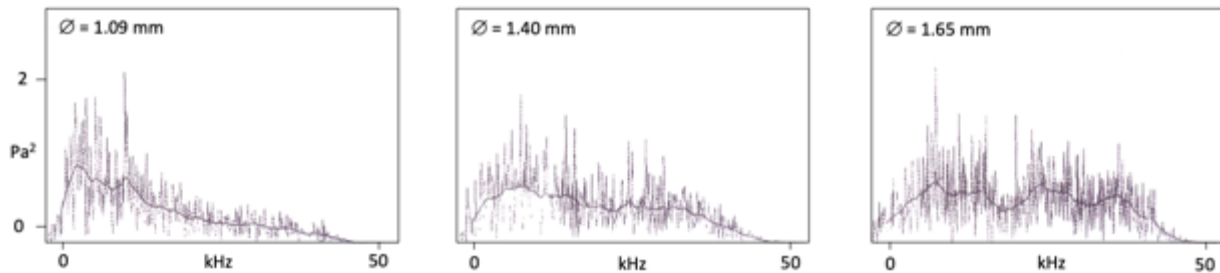**Figure 2. Power spectra of the vibration signals measured on the workpiece, with different focusers [15].**



**Figure 3. Power spectra of the acoustic signals measured with different focusers [22]; the continuous lines correspond to the ARMA estimates.**

## 2    Theoretical background

### 2.1    Vibration modes of a system

Each distributed body, herein referred to as system, is characterized by infinite vibration modes. A vibration mode is a harmonic oscillation of the system, in which potential energy is converted into kinetic energy and vice versa. A vibration mode is defined by its shape, frequency, and damping: the first is the oscillation pattern; the second is the oscillation frequency; the third is related with the attenuation versus time of the oscillation. The vibration modes are properties of the system and its constraints. Finite Element Method (FEM) models can be used for their numerical characterization. In the case of an undamped system with linear elastic behavior, the numerical problem reduces to the solution of the following eigenequation:

$$(K - \lambda \cdot M)\{\varphi\}$$

Here $K$ and $M$ are the stiffness and mass matrices of the mesh; the eigenvalues $\lambda$ and eigenvectors $\varphi$ correspond to the mode frequencies and mode shapes, respectively. The vibration modes of a system can also be characterized experimentally, by monitoring its forced response to a controlled excitation, as it will be pointed out in Section 2.2.

An unconstrained system is ideally suspended in void; hence, the correspondent vibration modes are only dependent upon its geometry and material properties. The unconstrained configuration is particularly relevant, as under such a status the system is isolated from its surrounding; hence, the modal characterization of the unconstrained system is often undertaken as preliminary step, before shifting the study to its real configuration, i.e. as part of an assembly.

## 2.2 Forced response of a system to an input excitation

If a harmonic excitation at a certain frequency is applied to one point of a system, its vibration occurs at the same frequency. The correspondent vibration shape is referred to as Operational Deflection Shape (ODS). The ODS is the weighted sum of the mode shapes, according to their respective frequency distances from the excitation; if the latter approaches a mode frequency, the ODS converges towards the correspondent mode shape. The vibration amplitude of a system is dependent upon that of the excitation; also, it tends to increase as the excitation frequency approaches a mode frequency and such phenomenon is known as resonance. A real excitation is typically non-harmonic, meaning that its spectrum is continuous and distributed over a certain frequency range; under this circumstance, and given the superimposition principle, the correspondent vibration spectrum occurs in the same frequency range.

Given a first point of a system, in which a harmonic excitation is applied, and a second point, in which the correspondent vibration is measured, the Frequency Response Function (FRF) is defined as the following [26]:

$$\text{FRF} = \frac{S_{xy}}{S_{xx}}$$

being $S_{xy}$ and $S_{xx}$ the cross-power between the excitation and vibration signals and the auto-power of the excitation signal, respectively. It follows that the FRF is a complex function of the frequency.

Impact testing is commonly used for experimentally characterizing a FRF. The method involves an impact excitation, which is provided by a hammer instrumented with a load cell at its tip; the excitation resembles a Dirac delta function, with its Power Spectrum (PS) being flat up to a certain cutoff frequency, then reducing to zero. The vibration response is measured, synchronously with the excitation; depending on the used sensor, the transduction can either be in displacement, velocity, or acceleration. Finally, the FRF is computed from the vibration and excitation signals; in a first approximation, it corresponds to the vibration spectrum, normalized by the excitation's amplitude, as shown in the example of Figure 4. Due to the presence of resonances, the FRF shows maxima in the correspondence of mode frequencies. As the cutoff frequency is approached, the cross-correlation between the two signals reduces and the FRF becomes noisier and less relevant.

The FRF provides data for the experimental characterization of a system's vibration modes: its resonant frequencies correspond to the mode frequencies; the width of each resonance can be used for assessing the correspondent modal damping. The assessment of the mode shape is also possible, by disposing of a set of FRFs at different measuring points: here the mode shape is the geometrical envelope, built on the imaginary amplitudes of the correspondent resonance, at the different measuring points.

## 2.3 Forced response of a system as means for diagnostics

Given one system, eventual geometrical changes due to wear progression affect its vibration modes, in particular the mode frequencies. In turn, the resonant frequencies of its forced response are affected, as well; hence, their monitoring is common practice in the field of machine diagnostics, as these correlate with the system's status. In general, two approaches are considered: monitoring the forced response to operational excitation; using a dedicated excitation, for triggering an adequate response. Of the two, the first approach is the most straightforward and compatible with day-to-day operations, as does not require dedicated setups and procedures.
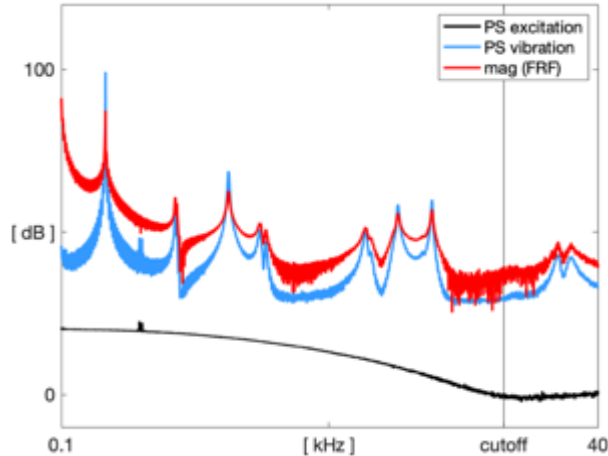
Figure 4. Example of FRF of a system (cantilever beam) and its experimental characterization by means of impact testing.

| Inner ⌀ | 1.02 mm |
|---|---|
| Outer ⌀ | 7.14 mm |
| Length | 101.60 mm |
| Material | Tungsten carbide |
| Mass density | 15.57 +/- 0.02 g/m3 |
| Young Modulus | 705 GPa |
| Roughness inner surface | < 1.4 µm Ra |

Table 1. Waterjet focuser – CERATIZIT Premium Line design.

## 3 Modal study of a waterjet focuser

### 3.1 Sensitivity of the focuser's mode frequencies to its wear progression

The present modal study applies to a standard waterjet focuser and is intended to assess the sensitivity of its mode frequencies to the wear progression. To the scope, two identical focusers have been considered, both CERATIZIT Premium Line design, for which the geometry and material properties are reported in Table 1. Of the two, one is new whilst the other has accumulated about 100 hours of operation; due to wear progression, its mass has reduced from 59.7 g to 56.6 g, at a rate of about 0.03 g/h; said material loss corresponds to an inner diameter's average increase from 1.02 mm to about 1.9 mm, without considering the actual uneven wear profile; the latter has been measured by means of destructive testing after the present study, and it is shown in the upper plot of Figure 5, for the sake of completeness.

An unconstrained configuration has been chosen for the specimens, mostly due to the requirement of isolating them from the surrounding; hence, it has been possible to investigate the vibration modes' sensitivities to the wear progression and disregard further interferential inputs, in particular the eventual constraint itself; indeed, the reproducibility of the latter would not be guaranteed, as the first specimen is removed from the test bench and replaced with the other.

The specimens' curved geometry prevents the installation of contact sensors on their external surfaces. Hence, a Laser Doppler Vibrometer (LDV) has been used, for the vibration measurements of this study. The bottom-left plot of Figure 5 shows the impact testing setup for the two specimens' FRFs characterization, and it includes: a foam layer, for supporting the specimens and providing unconstrained vibrating condition; an impact hammer (ENDEVCO 2301) for providing input excitation; a scanning LDV and its controller (POLYTEC PSV – 400), for measuring the vibration response; a data acquisition module (National Instruments CDAQ 9232), for signals' acquisition.



Figure 5. Upper plot: worn specimen's wear profile. Bottom-left plot: experimental setup for impact testing. Bottom-right plot: tested specimen and laser spot at its tip.

For each of the two specimens, an impact test has been carried out, consisting of five separate strikes. For each strike: the measurement point has been set nearby the focuser's tip and corresponds to the laser spot, as shown in the bottom-

right plot of Figure 5; the impact point has been chosen on the other specimen's end; the impact direction has been maintained aligned with the laser; the signals' acquisition has been carried out at a sampling frequency of 102.4 kHz and a recording period of 0.2 s; the acquisition trigger has been set on the hammer channel and a pre-trigger of 0.01 s has been used. The two FRFs have been computed as the arithmetic averages of the five correspondent strikes; the computation included the application of exponential decay windows to both the vibration and excitation signals. The results can be appreciated in the upper plots of Figure 6; the lower plots show the PSs of two excitation signals.
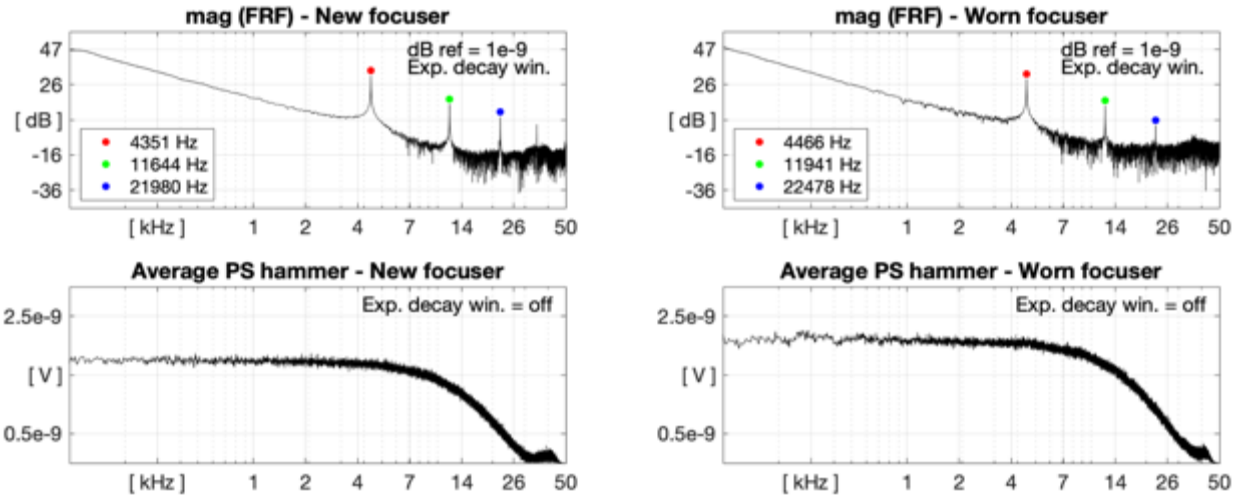


**Figure 6. Left plots: new focuser. Right plots: worn focuser. Upper plots: FRFs (magnitude). Lower plots: PSs of input excitations.**

The impacts' PSs appear flat up to about 10 kHz; above, they drop significantly and progressively reduce to noise level, at about 32 kHz; the anti-aliasing filter of the acquisition module starts at about 40 kHz and cuts higher contributions to zero. The FRFs are affected by high contributions in the low-frequency range; these rise to almost 47 dB and are due to rigid body motions of the unconstrained specimens, which are produced by the impacts; nonetheless, three resonances are clearly exhibited. The interpretation of this experimental data can be supported by a focuser's FEM study. The first three numerical modes are shown in Figure 7 and the following considerations stand: the first experimental resonance corresponds to the focuser's first bending mode; the second experimental resonance corresponds to the focuser's second bending mode; the third experimental resonance corresponds to the focuser's first torsional mode. The matching between the new focuser's experimental resonant frequencies and numerical mode frequencies is reported in Table 2.

The FEM model can also be used for investigating the mode frequencies' sensitivities to the wear progression: as the inner diameter is increased from 1.02 mm to 1.9 mm, the numerical mode frequencies increase as well; the reason for that is a trade-off between the reductions of mass, bending stiffness and torsional stiffness, with the first being dominant. Again, the numerical mode frequencies match their experimental counterparts, as it is shown in Table 3.
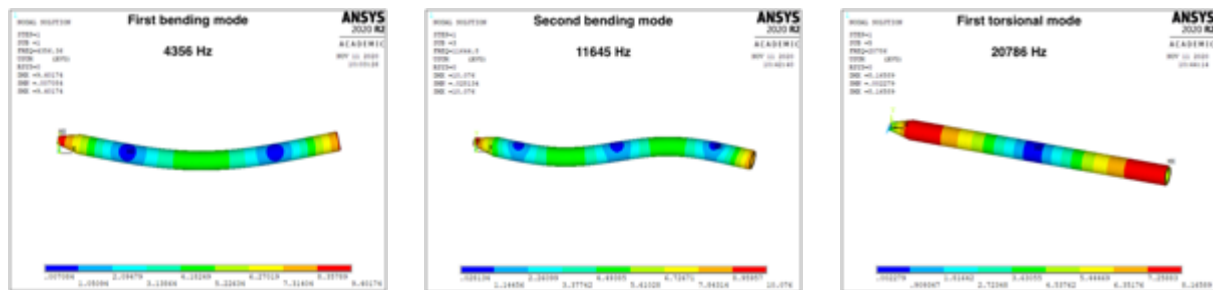


**Figure 7. Unconstrained focuser's numerical mode shapes.**

It should be mentioned that the FEM model does not catch the actual uneven wear profile of the inner bore; however, this approximation does not seem to compromise its accuracy, for the sake of this investigation.

The presented results indicate a relevant sensitivity (about 100 Hz) of the first mode frequency, to the wear accumulated by the focuser in about 100 hours of operation; hence, it seems possible to use such variable as a wear indicator. However, two further steps need to be addressed, before delivering final conclusions: the first is the

assessment of said mode frequency under the focuser's constraint of the AWJC system; the second is demonstrating that its in-line tracking is possible, by means of an operational vibration signal.

|  | Experimental | Numerical |
|---|---|---|
| Mode 1 | 4351 Hz | 4356 Hz |
| Mode 2 | 11644 Hz | 11645 Hz |
| Mode 3 | 21978 Hz | 20786 Hz |

**Table 2. New focuser's experimental resonances and numerical mode frequencies.**

|  | Experimental | Numerical |
|---|---|---|
| Mode 1 | 4466 Hz | 4476 Hz |
| Mode 2 | 11941 Hz | 11930 Hz |
| Mode 3 | 22478 Hz | 20805 Hz |

**Table 3. Worn focuser's experimental resonances and numerical mode frequencies.**

### 3.2    Assessment of the focuser's first mode frequency under the constraint of the AWJC system

The AWJC system used in the present investigation is an Intermac Primus 322 Metal installed at the Department of Mechanical Engineering of Politecnico di Milano (Italy); Figure 8 shows a focuser installed on the cutting head; the clamping is shown in Figure 00. The focuser's installation is carried out according to the following procedure: focuser's fitting with a tapered side nylon collet (8 mm height); focuser's pushing into the cutting head, against the mixing chamber; collet's pushing against the cutting head; tightening of the retaining flange. In such way, an interference fit is achieved, between the focuser and the cutting head. The focuser can be considered in a cantilever configuration; the clamp extends to 25 mm of the upper end, leaving only the 76 mm remaining portion free to vibrate; consequently, the vibration modes are expected to change, with respect to the unconstrained condition.
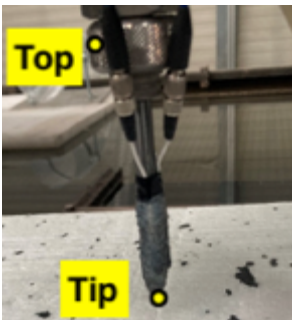


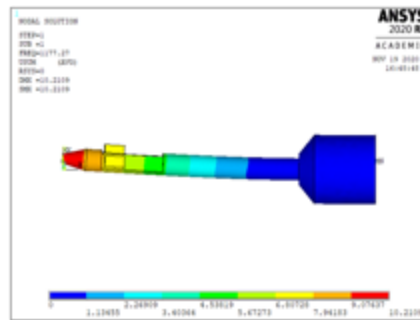**Figure 8. Focuser installed on the cutting head.**



**Figure 9. FEM prediction of the constrained focuser's first mode shape.**



**Figure 10. Specimen in a cantilever configuration.**

The FEM model represents an effective tool for providing an initial guess of the constrained focuser's first vibration mode. To the scope, the clamp has been reproduced by blocking the displacements of the mesh nodes involved. The numerical first mode shape is shown in Figure 9: again, it corresponds to a bending oscillation and the correspondent frequency is 1177 Hz, for the sound geometry; indeed, the first mode frequency in the cantilever configuration reduces with respect to the unconstrained configuration and coherently with the general beam theory [27]; as the inner diameter is increased to 1.9 mm, the first mode frequency's numerical prediction becomes 1221 Hz.

In order to provide experimental validation to the numerical data, the constrain has been reproduced on the new specimen, as shown in Figure 10: here the same specimen can be appreciated, as well as a steel adaptor and a steel plate for grounding, all the components glued together by means of LOCTITE 648. Indeed, the present setup has the benefit of reproducing the actual focuser's constraint on the AWJC machine, whilst reducing the number of inferential inputs from other components; this simplified configuration enables an easier interpretation of experimental results and provides guidance to the analysis of much more complex data from the real machine, as it will be pointed out in the following section. A second impact test has been carried out on the constrained specimen: the acquisition parameters and the number of strikes have been maintained the same, with respect to the previous study; the measurement point has been set nearby the focuser's tip and corresponds to the laser spot, as shown in Figure 10; the impact point has been chosen on the adaptor's top face; the impact direction has been maintained aligned with the laser. The computed FRF can be appreciated in Figure 11.

The FRF becomes much more complex, with respect to the free configuration; this is the consequence of further vibration modes of the ground plate and the adaptor, which are transmitted to the focuser as rigid oscillations. Hence, it becomes impossible to identify *a priori* the focuser's modes, among the larger set of resonances; furthermore, the focuser modes' amplitudes are not expected to dominate the overall response, due to the higher stiffness of its material, with respect to steel. The four dominant resonances are marked in the upper-left plot of Figure 11; these occur at the

frequencies of 109 Hz, 164 Hz, 394 Hz and 1165 Hz; the latter constitutes a good candidate for the constrained focuser's first mode frequency, considering its matching with the numerical prediction.

To confirm the previous hypothesis, a second impact test has been carried out, with the LDV used in a scanning configuration; here, the measurement spot has been moved across 25 points along the focuser's axis, whilst the impact point and direction have been maintained the same, as for the previous study; for each measurement point, five strikes have been carried out and the correspondent FRF computed, subsequently. Finally, the resulting set of 25 FRFs has been used for assessing the mode shapes associated to each of the four resonances. The results are shown in Figure 12: as it can be seen, the first three mode shapes are essentially combinations of rigid translations and rotations transmitted to the focuser, from the ground plate and the adaptor; on the other hand, the mode shape occurring at 1165 Hz corresponds to a bending oscillation pattern and appears consistent with the numerical prediction.
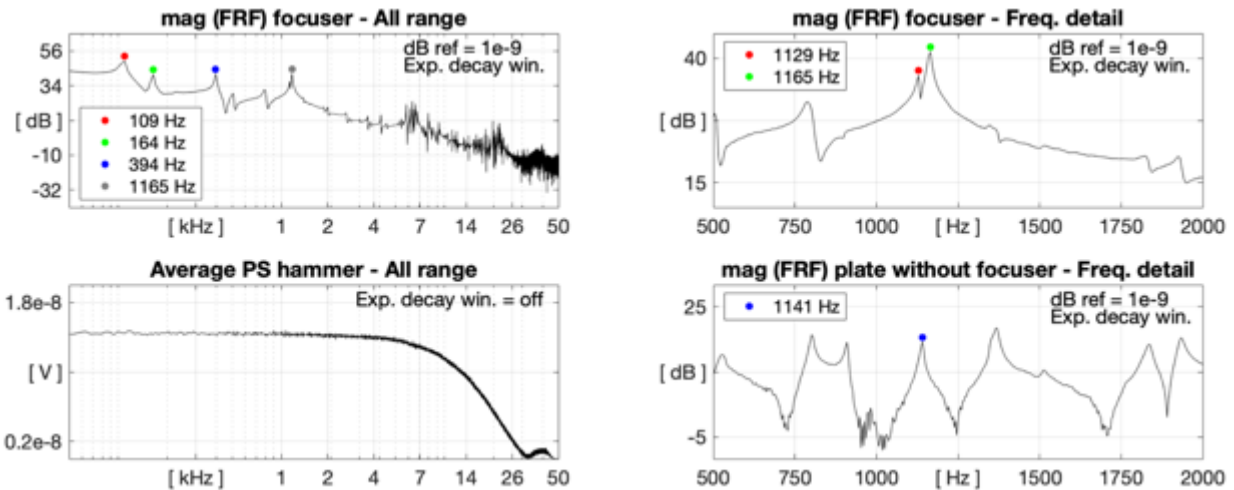


**Figure 11. Constrained specimen's FRF.**

A frequency detail is shown in the upper-right plot of Figure 11: here a further resonance at 1129 Hz can be appreciated, hence very close the one identified as the focuser's first mode frequency. To explain its presence, a further impact test has been carried out: here the focuser has been removed and the LDV pointed at the plate, in the proximity of the adaptor; the impact point has been maintained on the adaptor's top face. The resulting FRF is shown in the bottom-right plot of Figure 11: here one resonance appears, at the frequency of 1141 Hz; this resonance is obviously associated to one vibration mode of the plate, as the focuser is not present; once the focuser is installed, the correspondent frequency reduces to 1129 Hz, due to the added mass; at the same time, the focuser's mode appears at 1165 Hz.
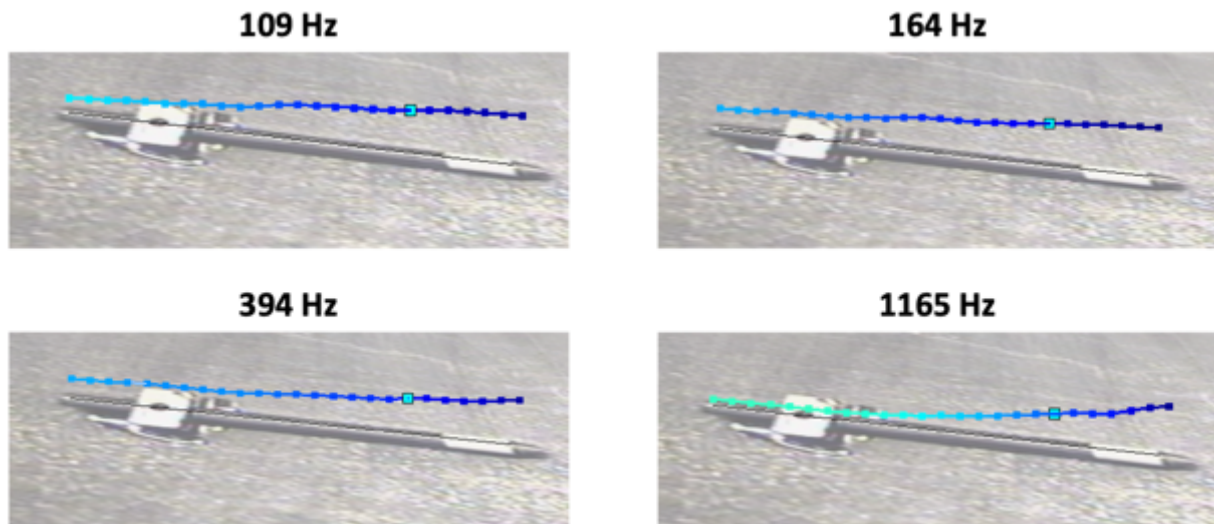


**Figure 12. Constrained specimen's experimental mode shapes.**

# 4        In-line monitoring of the focuser's first mode frequency during operation

The present investigation made use of a CERATIZIT Premium line focuser with special geometry, which has been kindly provided by the manufacturer. The focuser is shown in Figure 13 and here the following features can be appreciated: two orthogonal flat areas, which have been machined on the external surface and nearby the tip, before sintering; two micro-accelerometers (DYTRAN 3224A), which have been attached to each flat area by means of LOCTITE 648; the accelerometers' technical specifications are reported in Table 4. The authors have used the same focuser in another investigation [25], which explains the reason for having two onboard accelerometers, despite only one is required by the present study.



**Figure 13. Focuser with special geometry and onboard accelerometers.**

| Mass | 0.2 g |
|------|-------|
| Sensitivity | 10 mV/g |
| Range | 2 Hz to 20 kHz |
| Resonance | > 95 kHz |

**Table 4. Technical specifications DYTRAN 3224A.**

As a first step, an impact test has been carried out on the focuser installed on the AWJC machine, in order to verify the presence of a resonance at the frequency expected by the previous study: to the scope, two impact points have been considered, one at the focuser's tip and the other on the clamp; the two impact points are indicated in Figure 8 with the "*tip*" and "*top*" labels, respectively; five strikes have been carried out, for each impact point; the vibration has been monitored by means of one of the two accelerometers; the acquisition parameters and computation methods have been maintained the same as for the previous impact tests. The tip and top FRFs can be appreciated in Figure 14: these appear even more complex with respect to Figure 11, due to the presence of vibrating modes of further machine components, which are triggered by the strikes and transmitted through the clamp, as focuser's rigid oscillations; however, the tip FRF clearly exhibits one resonance at 1172 Hz, which closely matches the expected value, hence can be licitly assumed as the installed focuser's first mode frequency; this assumption is corroborated by the fact that the same resonance is less pronounced on the other FRF and coherently with the focuser's lower sensitivity to the top strikes.
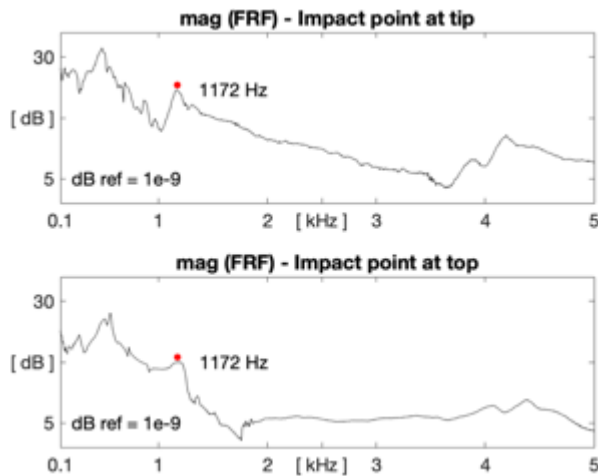


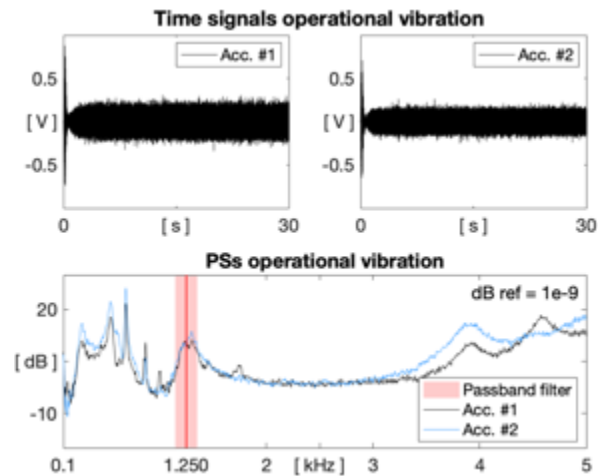**Figure 14. FRFs of the focuser installed on the AWJC machine.**



**Figure 15. Operational vibration signals delivered by the accelerometers.**

As a further step, the possibility of tracking the focuser's first mode frequency by means of operational excitation has been assessed. To the scope, the abrasive waterjet has been fired for 30 s, while maintaining the head steady and without workpiece; the water pressure and the abrasive feed rate have been set to 330 MPa and 300 g/min, respectively; a Barton Garnet, Mesh 80 abrasive has been used. The NI9232 module has been used for the signals' acquisition of the two accelerometers; the sampling frequency and recording period have been set to 102.4 kHz and 30 s, respectively; the trigger has been set on one accelerometer's channel and a pre-trigger of 0.1 s has been used. The upper plots of Figure 15 shows the vibration signals in the time domain; due to the absence of a reference excitation

signal, the processing has been limited to a PS computation by means of the Welch's method [28] (steady chunk, 100 averages, no overlap, hamming window). The result can be appreciated in the lower plot of Figure 15: here, the resonance associated with the focuser's first vibration mode is still visible; its peak appears wider and slightly shifted towards higher frequencies, at about 1250 Hz, due to the presence of a high-speed waterjet inside the focuser, which is expected to increase its bending stiffness. The resonance is well detected by both accelerometers, as expected to happen unless the unfortunate case in which the bending oscillation occurs perfectly orthogonally with respect to one of the two sensors' sensitivity direction. Hence, only the first accelerometer has been considered for the subsequent part of this study.
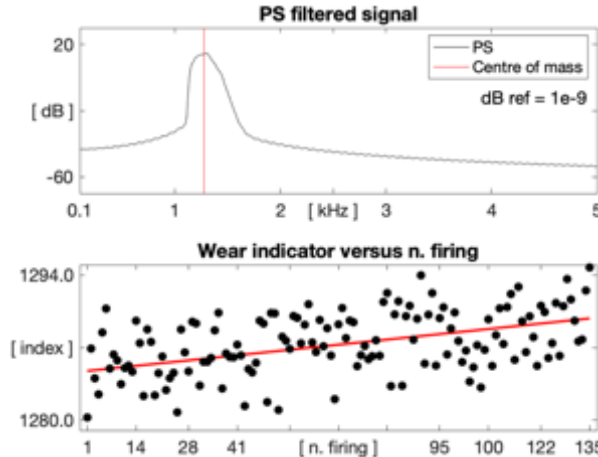


Figure 16. Filtered signal's PS and wear indicator vs. firing number of the factorial study.
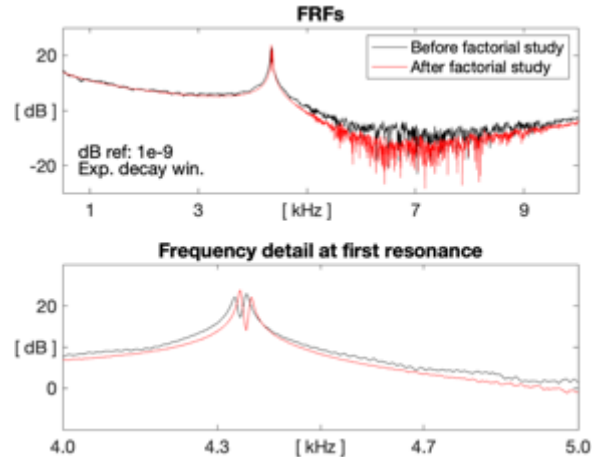


Figure 17. Unconstrained focuser's FRFs before and after the factorial study.

The resonance associated with the focuser's first vibration mode appears distributed over a wide frequency range, hence the need for a more robust tracking method, with respect to the simple maximum picking. So, the following processing method has been applied to the accelerometer's time signal: passband filter (centre: 1250 Hz; width: 200 Hz), as shown in the lower plot of Figure 15; filtered signal's PS computation, whose result is shown in the upper plot of Figure 16; computation of the focuser's first mode frequency as the centre of mass of the filtered signal's PS, as shown in the upper plot of Figure 16.

Due to its sensitivity to the wear progression, the first mode frequency is expected to gradually shift towards higher values, as operating hours are accumulated by the focuser; hence, this variable can be used as the indicator of its wear status. On this regard, the present focuser has been used in an analogous factorial study to the one discussed in [25], which overall involved 135 firings of the waterjet, each one of the duration of 30 s, and the acquisition of the correspondent accelerometer's signal; the study equals to a total amount of about 4050 s of operation, which are not sufficient for bringing the focuser to a complete worn status, but could be sufficient for producing a detectable indicator's shift. Indeed, the lower plot of Figure 16 shows the correspondent indicator computed for each firing, and an upward trend is clearly exhibited; the red line is an interpolation of the experimental data points and indicates a total indicator's shift of about 5 Hz by the end of the factorial study, with respect to the initial value. The trend's statistical relevance is confirmed by the Mann-Kendall test [29], for a confidence level greater than 99 %. The experimental data's standard deviation with respect to the fitting line is 2.3 Hz; hence, the total indicator's shift of 5 Hz corresponds to a 97.2 % coverage factor; given that, the present method appears capable of delivering a reliable wear indicator, about every hour of operation.

As a last step, the focuser has been dismounted from the machine and the two accelerometers removed. Weigh of the specimen indicates a material loss of 0.05 g during the factorial study, which is coherent with the rate esteemed in Section 3.1. Subsequently, an impact test has been carried out on the specimen, under the same unconstrained condition and setup of Section 3. The computed FRF can be appreciated in Figure 17; here it is also shown the comparison with an analogous impact test that has been carried out on the same unconstrained specimen, but before the factorial study; the comparison confirms a detectable sensitivity (about 12 Hz for the unconstrained configuration) of the focuser's first mode frequency to the wear accumulated in one hour and a half of operation; as a last note with regard to Figure 17, it should be mentioned the splitting of the first mode into two close but separate resonances, due to the presence of the flat areas on the specimen, which introduce a slight axial asymmetry. Both the weight loss and the measured resonance's shift in the impact tests confirm the correlation of operational data with wear progression,

whilst further inferential inputs like the jet interaction with the specimen do not seem to substantially affect the method and conclusions.

## Conclusions

The present investigation demonstrated the possibility of inline monitoring a waterjet focuser's wear progression, by means of its operational vibration. This conclusion was made possible by means of two separate studies, of which the first was intended to demonstrate an adequate sensitivity of the focuser's mode frequencies to its wear status, whilst the objective of the second was to prove the possibility of inline tracking the first mode frequency from the operational vibration signal delivered by an accelerometer installed at the focuser's tip. The proposed method makes use of low-cost and non-invasive sensing hardware, which can be easily retrofitted into a focuser's design. Its deployment in a real production environment is expected to tackle end-user requirements for improved process robustness and automation, by delivering a reliable indicator of the focuser's residual life, as well as by overcoming the requirement for constant human supervision over its status.

## Declarations

### Funding

### Competing interests

The authors declare that they have no known competing financial interests or personal relationships that could have appeared to influence the work reported in this paper.

### Availability of data and material

The data that support the findings of this study are available on request from the corresponding author.

### Code availability

The code that supports the findings of this study is available on request from the corresponding author.

### Authors' contributions

The listed coauthors have provided substantial contributions to the present investigation.

### Ethics approval

Not applicable.

### Consent to participate

Not applicable.

### Consent to publication

Not applicable.

### Notes and acknowledgements

The systems and methods for monitoring the operational vibration and delivering the wear indicator from the signals are the objects of five patent applications [30][31][32][33][34]. The intellectual property included in said patents belongs to the University of Luxembourg.

## References

[1]. J. Folkes, "Waterjet – an innovative tool for manufacturing", *Journal of Materials Processing Technology*, vol. 209, pp. 6181-6189, 2009. DOI: 10.1016/j.jmatprotec.2009.05.025

[2]. D. A. Summers, "Waterjetting Technology", *E & FN Spon*, 1995, London, England.

[3]. A. W. Momber, R. Kovacevic, "Principles of Abrasive Water Jet Machining", *Springer*, 1998, Berlin, Heidelberg, New York.

[4]. J. Wang, "Abrasive Waterjet Machining of Engineering Materials", *Trans Tech Publications Ltd.*, 2003, Switzerland.

[5]. M. Hashish, "Cutting with abrasive waterjets", *Mechanical Engineering*, vol. 106 (3), pp. 60-69, 1984. ISSN: 00256501

[6]. S. Garg, "Waterjet cutting machine market", *Markets and Markets*, 2018.

[7]. H. T. Liu, "Waterjet technology for machining fine features pertaining to micromachining", *Journal of Manufacturing Processes*, vol.12 (1), pp. 8-18, 2010. DOI: https://doi.org/10.1016/j.jmapro.2010.01.002

[8]. M. Putz, M. Dittrich, M. Dix, "Process Monitoring of Abrasive Waterjet Formation", *Procedia of the 7th HPC 2016 – CIRP Conference on High Performance Cutting*, vol. 46, pp. 43-46, 2016. DOI: 10.1016/j.procir.2016.03.189

[9]. M. Annoni, F. Arleo, F. Viganò, 2017, "Micro-waterjet Technology", in: Fassi I., Shipley D. (eds) Micro-Manufacturing Technologies and Their Applications. Springer Tracts in Mechanical Engineering, pp. 129-148.

[10]. G. Pozzetti, B. Peters, "A numerical approach for the evaluation of particle-induced erosion in an abrasive waterjet focusing tube", *Powder Technology*, vol. 333, pp. 229-242, 2018. DOI: http://dx.doi.org/10.1016/j.powtec.2018.04.006

[11]. M. Hashish, "Observations of wear of abrasive-waterjet nozzle materials", *Journal of Tribology*, vol. 116 (3), pp. 439-444, 1994. DOI: https://doi.org/10.1115/1.2928861

[12]. M. Nanduri, D. G. Taggart, T. J. Kim, "The effects of system and geometric parameters on abrasive water jet nozzle wear", *International Journal of Machine Tools and Manufacture*, vol. 42 (5), pp. 615-623, 2002. DOI: https://doi.org/10.1016/S0890-6955(01)00147-X

[13]. M. Nanduri, D. G. Taggart, T. J., Kim, "A study of nozzle wear in abrasive entrained water jetting environment", *Journal of Tribology*, vol. 122 (2), pp. 465-471, 2000. DOI: 10.1115/1.555383

[14]. A. Perec, F. Pude, A. Grigoryev, M. Kaufeld, K. Wegener, A study of wear on focusing tubes exposed to corundum-based abrasives in the waterjet cutting process", *The International Journal of Advanced Manufacturing Technology*, vol. 104 (5), pp. 2415-2427, 2019. DOI: 10.1007/s00170-019-03971-0

[15]. P. Hreha et al., "Monitoring of focusing tube wear during abrasive waterjet (AWJ) cutting of AISI 309", *Metalurgija*, vol. 53 (4), pp. 533-536, 2014. ISSN: 0543-5846

[16]. R. Kovacevic, "A new sensing system to monitor abrasive waterjet nozzle wear", *Journal of Materials Processing Technology*, vol. 28 (1–2), pp. 117-125, 1991. DOI: https://doi.org/10.1016/0924-0136(91)90211-V

[17]. T. Susuzlu, "Development and evaluation of ultra high pressure waterjet cutting", Ph.D. thesis, Delft University of Technology, 2008. ISSN: 9789090230757

[18]. J. Ion, "Laser processing of engineering materials – principles, procedure and industrial application", *Elsevier*, 2005, Oxford, England. ISSN: 0 7506 6079 1

[19]. S. M. Bangu, M. Coteata, "Plasma arc cutting cost", *International Journal of Material Forming*, vol. 2, pp. 689-692, 2009. DOI: DOI: http://dx.doi.org/10.1007/s12289-009-0588-4

[20]. M. Bauer, O. Grünzel, H. J. Maier, T. Hassel, "Full automation of waterjet cutting", 2017 WJTA-IMCA Conference and Expo, October 25-27, 2017, New Orleans (US)

[21]. C. Cempel, "Vibroacoustical diagnostics of machinery: an outline", "Mechanical Systems and Signal Processing", vol. 2 (2), pp. 135-151, 1988. DOI: https://doi.org/10.1016/0888-3270(88)90039-8

[22]. R. Kovacevic, L. Wang, Y. M. Zhang, "Identification of abrasive waterjet nozzle wear based on parametric spectrum estimation of acoustic signal", *Proceedings of the Institution of Mechanical Engineers, Part B:*

*Journal of Engineering Manufacture*, vol. 208 (3), pp. 173-181, 1994. DOI: https://doi.org/10.1243/PIME_PROC_1994_208_076_02

[23].    R. Kovacevic, L. Wang, Y. M. Zhang, "Detection of Abrasive Waterjet Nozzle Wear Using Acoustic Signature", Proceedings of the American Waterjet Conference, vol. 7, pp. 217-232, 1993

[24].    R. Kovacevic, M. Evizi, "Nozzle wear detection in abrasive waterjet cutting systems", *Materials Evaluation*, vol. 48 (3), pp. 348-353, 1990

[25].    E. Copertaro, F. Perotti, P. Castellini, P. Chiariotti, M. Martarelli, M. Annoni, "Focusing tube operational vibration as a means for monitoring the abrasive waterjet cutting capability", *Journal of Manufacturing Processes*, vol. 59, pp. 1-10, 2020. DOI: https://doi.org/10.1016/j.jmapro.2020.09.040

[26].    D. J. Ewins, "Modal Testing: Theory and Practice", *John Wiley & Sons Inc.*, 2009. ISBN: 9780863802188

[27].    C. F. Beards, "Structural Vibration: Analysis and Damping", *John Wiley & Sons Inc.*, 1996. ISBN: 9780080518053

[28].    P. D. Welch,, "The use of Fast Fourier Transform for the estimation of power spectra: A method based on time averaging over short, modified periodograms", *IEEE Transactions on Audio and Electroacoustics*, vol. 15 (2), pp. 70-73, 1967. DOI: 10.1109/TAU.1967.1161901

[29].    H. B. Mann, "Nonparametric tests against trend", *Econometrica*, vol. 13 (3), pp. 245-259, 1945. DOI: https://doi.org/10.2307/1907187

[30].    E. Copertaro, "Wear monitoring device and process for an abrasive waterjet cutting head", Luxembourg national patent application No. LU100936, filing date 26 September 2018.

[31].    E. Copertaro, "Wear monitoring device and process for an abrasive waterjet cutting head", PCT patent application No. PCT/EP2019/076119, filing date 26 October 2019, publication date 2 April 2020.

[32].    E. Copertaro, "Machining system and monitoring method", Luxembourg national patent application No. LU101065, filing date 21 December 2018.

[33].    E. Copertaro, "Machining system and monitoring method", PCT patent application No. PCT/EP2019/086911, filing date 23 December 2019, publication date 25 June 2020.

[34].    E. Copertaro, Waterjet focuser with DMS sensors for monitoring operational vibration and delivering an index of residual life, Luxembourg national patent application No. LU102298, filing date 16 December 2020.